vetmeduni

Final (research) report regarding the Marshall Plan Foundation Scholarship 2020

Computed tomographic features of primary lung tumors in dogs and cats

Dr. med. vet. Carina Strohmayer DipECVDI
Diagnostic Imaging, Vetmeduni

Acknowledgment

First, I want to thank the Marshall Plan Foundation for this opportunity. Fostering interinstitutional exchange and collaboration is most valuable for knowledge transfer and building a scientific long lasting network.

Moreover I am grateful for the support of Ao.Univ.-Prof. Dr.med.vet. Sibylle Kneissl from my home university. She always finds a solution for a problem and contributes innovative ideas.

I want to thank Agustina Anson DVM, PhD, DECVDI from the host university (Tufts University, Cummings School of Veterinary Medicine). I am very grateful for this collaboration and continuous exchange on all levels. Muchas gracias!

Last but not least I want to thank all involved colleagues for their technical support!

Table of contents

1 Abstract

Computed tomography (CT) is important for diagnosing, surgical planning and monitoring of lung tumors in dogs and cats, yet more advanced CT features are lacking. In this retrospective multicenter study, 68 dogs and 21 cats were included. The project was conducted considering mitigation circumstances of COVID-19 at the time of the study. A pilot study with nine dogs was conducted to evaluate a CT evaluation scheme. The evaluated CT parameters included the affected lung lobe, distribution, shape, margination, contact to pleura, dimensions and attenuation. Characteristics of the involved bronchi and vessels were assessed. Additionally, the presence of intralesional gas and/or mineralization, pulmonary nodules, pleural effusion and assessment of tracheobronchial lymph nodes was reported. In a next step the entire study population will be evaluated by three reviewers in consensus.

2 Introduction

The aim of the project was to describe CT characteristics of lung tumors in dogs and cats in more detail and with a representative study population since the last larger imaging studies are approximately a decade ago. To achieve this, increasing the study population by a multicenter study was anticipated. Retrospectively archives from multiple universities were therefore searched for lung tumors with histopathological diagnosis. Due to the COVID-19 pandemic which was in effect with great consequences at the time when the PhD student was planning to go the United Stated of America for the exchange program, lead to the solution of remotely performing the project.

3 Background

3.1 Lung tumors in veterinary medicine

3.1.1 Incidence and risk factors

Domestic animals concurrent to their owners show an increasing life span, posing demand on veterinary medicine to scientifically account for more investigation on prognosis and oncologic treatment (Cozzi et al. 2017). The incidence of primary lung tumors in dogs and cats is fortunately reported to be low, however current data are sparse (D'Costa et al. 2012, Dobson et al. 2002).

The mean age with primary lung tumors is reported with 11.30 ± 1.99 years and 13.8 years respectively in dogs and cats (Rose and Worley 2020, Santos et al. 2022). The majority of cats with pulmonary carcinoma are usually older than 10 years (Santos et al. 2022). Described predominant breeds include Domestic Shorthair with about 80% followed by Persian, Siamese and Himalayan cats (Santos et al. 2022). In dogs, various breeds are reported without a statistical significance (Rose and Worley 2020). Tobacco smoke exposure or inhalation of polluted air are environmental risk factors in the development of lung tumors in human medicine, however this etiology has not been clearly demonstrated in animals (Culp and Rebhun 2020a).

3.1.2 Clinical Signs

Up to 30% of lung tumors are diagnosed incidentally through routine geriatric screening. Those patients with clinical signs most commonly present with cough as leading complaint. Other clinical signs reported include exercise intolerance, inappetence, dyspnea, lethargy, hyporexia,

weight loss, or hemoptysis (Rose and Worley 2020; Culp and Rebhun 2020a; Polton et al. 2018; Aarsvold et al. 2015). Uncommonly, lameness is also described in patients with lung tumors. Causes may be attributed to periosteal reaction along the axial skeleton secondary to hypertrophic osteopathy mainly in dogs (Withers et al. 2015) or bone metastases to phalanges in cats (Goldfinch and Argyle 2012). Hypertrophic osteopathy is an uncommon pathologic disease process accounting for diffuse periosteal new bone formation along the limbs. It occurs due to mainly neoplastic but also infectious diseases, however the pathogenesis has not been fully resolved (Cetinkaya et al. 2011). In cats, lameness has been reported due to bone metastasis of lung tumors to the phalanges. This entity is known as 'feline lung–digit syndrome' (Goldfinch and Argyle 2012).

3.1.3 Pathology

Primary lung tumors can arise from epithelial tissues of the conducting airways and alveolar parenchyma or can be of mesenchymal origin. Most commonly tumors are of epithelial origin.

Epithelial tumors

Tumors of the large airway epithelium are more frequently close to the hilar region in the lung, while tumors arising from the alveolar parenchyma are more likely to be peripheral.

There are multiple approaches to classify lung tumors based on the tissue of origin (bronchogenic, bronchioalveolar,…), the histologic pattern (lepidic, papillary, acinar, squamous, adenosquamous.) or a combination. The classification system used is not uniform and often varies slightly between institutions.

Concerning the histologic subtypes, a lepidic pattern or bronchioloalveolar tumor pattern is defined as cuboidal to slightly flattened epithelial monolayers, which are lining alveolar-like structures (Wilson 2017c). Interestingly the term bronchioloalveolar tumors is controversially discussed. A clear assignment to a bronchoioalveolar type is based on the presence of alveolar-like septae lined by cuboidal epithelial cells which is described in the pattern as "lepidic." Therefore, bronchioloalveolar tumors are allocated best being classified as adenocarcinoma in situ (Wilson 2017b).

A papillary pattern on the other hand is characterized by branching and exophytic growths, infiltrating spaces larger than normal alveoli (Wilson 2017c). An acinar pattern describes a glandular growth with more connective tissue as well as central lumen containing mucus (Wilson 2017d). Besides those types, a squamous pattern consists of solid accumulations of cells and eosinophilic cytoplasm which is resembling nonkeratinizing stratified epithelium (Wilson 2017e).

In dogs, primary lung tumors most commonly arise from the terminal bronchiolar alveolar regions. Carcinoma is the most common described tumor type with adenocarcinoma most prevalent. In a large study with 340 dogs, papillary adenocarcinoma made up the biggest proportion with 32%, while the second most common type with 13% was diagnosed as bronchoalveolar adenocarcinoma. Other epithelial tumors were adenosquamous and squamous carcinoma in 4% and 2% respectively. Primary pulmonary histiocytic sarcoma was diagnosed in 6% (McPhetridge et al. 2022). Occurrence of different or confluent patterns can often be seen in different regions of the tumor. In another study of 40 dogs, the authors reported bronchoalveolar carcinoma as the most common tumor with 36%, followed by papillary pulmonary carcinoma with 27% and adenosquamous carcinoma with 18% (Rose and Worley 2020). Those different percentages in sub-classification demonstrate the current differences in histologic grading.

In cats, the most common primary tumor is the adenocarcinoma with 60-70% (Wilson 2017a). The most common locations are the caudal lung lobes. A recent study described three gross patterns of the pulmonary tumors, namely a large nodule with additional smaller nodules in 62%, a solitary nodule in 26% and small, multifocal to coalescent nodules in 13%. Concurrent pathological findings in this study included atelectasis, hydrothorax, pleural adhesions or bronchial compression. Authors of the same publication used a modified and simplified histological classification with no reference to the cell of origin. They graded the tumors in adenocarcinoma, adenosquamous carcinoma (ADS), and squamous cell carcinoma (SCC). A sub-classification of adenocarcinoma based on the subjective evaluation of the predominant glandular growth pattern in lepidic, acinar, papillary, micropapillary, and solid was conducted. Half of the 39 cases were graded as papillary adenocarcinoma. The terms “adenocarcinoma in situ,” “minimally invasive adenocarcinoma,” and “invasive adenocarcinoma” commonly used in humans and dogs were not applied due to inconsistent definitions, including the relationship between tumor size and histological characteristics as well as the size of foci of invasive lesions with reported survival times for cats. Based on their results pulmonary tumors ≤ 3 cm showed in nearly 40% extrapulmonary metastases and demonstrated at least one invasive component. Interestingly no SCC was diagnosed. They discussed as well that a glandular and squamous patterns of ≥10% for classifying a tumor as ADS, might have influenced the evaluation (Santos et al. 2022).

Mesenchymal tumors

Histiocytic sarcoma

Histiocytic sarcoma originates from interstitial dendritic cells and can occur locally in spleen, lymph nodes, lung, bone marrow, skin/subcutis, brain, and articular tissues of appendicular joints or present as a disseminated disease (Moore 2017a). Reported predisposed breeds include Bernese Mountain Dog, Rottweiler, Golden Retriever and Flat-Coated Retriever (Moore 2017b). The characteristics of pulmonary histiocytic sarcoma do not differ from other organs. In the presence of a pulmonary mass other sites should be evaluated for a multicentric disease (Wilson 2017f).

Pulmonary lymphoma / Angiocentric B-cell lymphoma with reactive T cells (lymphomatoid granulomatosis)

The lung is a rare location for lymphoma. It can manifest as one or more masses or diffusely surrounding blood vessels of normally appearing lung (Valli et al. 2017). Leite-Filho et al. (2018) showed in 16/125 (13%) necropsy cases of cats lung infiltration by lymphoma. In a quarter of the cats, masses were noted, followed by nodules in a fifth. Interestingly the majority consisting of nearly 60% did not present with any gross changes. Histologically the most common pattern was a peribronchial-vascular infiltration. 75% showed more than one pulmonary infiltration pattern. Most of the cases were diagnosed as B-cell and less than 15% were diagnosed as T-cell lymphoma. A proportion of cats were also positive for the feline leukaemia virus and feline immune-deficiency virus.

3.1.4 Diagnostic imaging

Diagnostic imaging is essential for the diagnosis and planning of pulmonary tumors. While thoracic radiography is the first line modality in detecting a pulmonary mass, computed tomography (CT) got more widely available and is considered the gold standard in veterinary diagnostic imaging of the lung.

CT articles about lung tumors in dogs and cats are limited and recent papers are lacking. One large imaging study about feline primary lung tumors from Aarsvold et al. (2015) included 57 cats. Most of the tumors were adenocarcinomas, while 11% tumors were of bronchial origin, 5% were adenosquamous cell carcinoma and 2% squamous cell carcinoma. They described the presence of a pulmonary mass in 96% while in 4% a disseminated pulmonary lesion with no defined mass was seen. A contact with the visceral pleural was noted in almost all cases. The margins were irregular and well defined in approximately 80%. In about three quarter of the cases bronchial compression and in a fifth of the cases bronchial infiltration was seen. Gas-

containing cavities were noted in about 60% and foci of mineral attenuation were seen in slightly more than half of the cats. Pulmonary nodules suggestive of metastasis were detected in 50%. Pleural effusion was present in 30% and pulmonary thrombosis in approximately 10%. The mean maximal dimension of pulmonary masses was 3.5 cm with a range of 1.1-11.5 cm. The authors did not find a correlation between tumor type and CT findings.

The largest imaging study on primary pulmonary tumors in dogs to date was carried out by Marolf et al. (2011) including 17 carcinomas and two sarcomas. All pulmonary masses were bronchocentric and showed an air bronchogram. The affected bronchi were narrowed, displaced as well as frequently obstructed by the tumor. Besides one pneumonic/alveolar form, all other masses were solitary. The majority of solitary masses were well circumscribed, detected in a cranial or caudal lobe and displayed a mild to moderate heterogeneous contrast enhancement. In 26% of the dogs there was evidence of pulmonary metastasis and in about a fifth of the cases tracheobronchial lymphadenopathy was identified. Mineralization of the mass was noted in only three out of 19 dogs.

Recently a case series of CT characteristics of cavitary pulmonary adenocarcinoma has been described in three dogs and two cats. They reported findings such as lobular and spiculated margins, air bronchograms, heterogeneous contrast enhancement, as well as pleural tags, and ground-glass opacity in close proximity to the mass (Parry et al. 2021). Another study focused on neoplastic transformation of cystic airspaces. Features were thickening or irregularity of the wall, adjacent soft-tissue nodules or solid and non-solid tissue mixed within clusters of multiple cystic airspaces. The authors therefore recommend monitoring cystic airspace lesions. They proposed an adapted classification for tumors associated with cystic airspaces. Type I describes a soft tissue nodule associated with the outer limits of the cystic airspace. Type II represents a soft tissue nodule extending into the cystic airspace from the wall. Type III is classified as cyst wall thickening without an association with soft tissue nodules. And type IV is a complex lesion with multiple cysts and soft-tissue components (Bello et al. 2021).

Apart from carcinomas, a CT study about intrathoracic histiocytic sarcoma in dogs reported intrathoracic lymphadenopathy and pulmonary masses as the most common findings. Regarding the lymph node involvement, a sternal and tracheobronchial lymphadenopathy was more common than cranial mediastinal lymphadenopathy. Concerning pulmonary masses, there was predilection for the right middle lung lobe and a ventral distribution was seen in the majority of cases. Most of the masses showed mild to moderate heterogeneous enhancement and were poorly marginated and bronchocentric (Tsai et al. 2012).

On the other hand only a radiographic study about imaging findings of the rare pulmonary lymphoma in seven cats and 16 dogs exist. Radiographic findings included a wide range from the absence of an abnormal pattern, to alveolar, unstructured interstitial infiltrates, nodules or masses and bronchial infiltrates. The authors described also pleural effusion and lymphadenopathy (Geyer et al. 2010). CT descriptions of pulmonary lymphoma in veterinary domestic animals are lacking.

Evaluating the regional lymph nodes is critical as the presence of lymph node enlargement might indicate the presence of metastasis and guides sampling. The tracheobronchial lymph nodes are located one on each side of the tracheal bifurcation and a third one in between the main stem bronchi. In dogs, likely metastatic involvement has been proposed with a cut-off ratio (lymph node to thoracic body ratio of 1.05) and an absolute measurement (transverse maximum lymph node diameter of 12 mm). Besides also a heterogenous and/or ring pattern was attributed to metastatic disease (Ballegeer et al. 2010). In cats, only the CT appearance of normal tracheobronchial lymph nodes has been published. The authors described 1.7, 2.4 and 2.7 mm as mean height, width and length respectively (Smith et al. 2020).

3.1.5 Treatment and Prognosis

Interestingly in a recent study in cats, a primary lung tumor was considered the reason of death in only over 65% of the cases. Concurrent disease of those cats consisted of chronic renal disease or intestinal lymphoma. Extrapulmonary metastatic sites were noted in 56.4% and included the reginal lymph nodes, skeletal muscles, pleura, kidney, dermis/subcutis and the eyes (Santos et al. 2022).

In dogs, multiple factors influencing the prognosis have been described. The presence of clinical signs, histologic features, degree of primary tumor extension, residual disease after surgical, pulmonary metastatic disease and the influence of locoregional lymph node involvement have been addressed (McNiel et al. 1997, Ogilvie et al. 1989, Rose and Worley 2020). Rose and Worley concluded that the median survival time of dogs with lymph node metastasis was approximately 5.5 months. Additionally, they reported that dogs with a tumor size of > 100 cm^3 and nodal metastasis had a shorter survival time in comparison to dogs with a tumor of similar size and no evidence of lymph node metastasis. Therefore, assessing the lymph node size during pre-surgical CT is important. However, lymph node metastasis can be presence in the absence of lymph node enlargement. In this study three out of 11 dogs with lymph node metastasis did not show lymph node enlargement evident on CT. Therefore, to

properly stage the patient it is recommended to acquire lymph node biopsy at the same time as lung lobectomy (Rose and Worley 2020).

The surgical method of choice is considered lobectomy. Data on efficacy of chemotherapy is limited and reported in terms of unresectable or metastatic tumors. In a study about dogs with advanced (metastatic) primary lung carcinoma who were treated by metronomic chemotherapy demonstrated a measurable clinical benefit together with no significant risk or toxicity (Culp and Rebhun 2020b, Polton et al. 2018). Another study showed a favorable prognosis of dogs with primary pulmonary histiocytic sarcoma treated with curative-intent surgery and adjuvant systemic chemotherapy with lomustine (Murray et al. 2022).

4 Materials and Methods

In the beginning the patient information systems of the University of Veterinary Medicine, Vienna (Vetmeduni) as home university, the Tufts University, Cummings School of Veterinary Medicine and the College of Veterinary Medicine, North Carolina (NC) State University as collaboration partners were searched for the inclusion criteria.

Inclusion criteria consisted of thoracic CT with at least one post contrast series and a histopathological diagnosis of a lung tumor in dogs and cats.

Retrieving patients

To retrieve cases from Vetmeduni, thoracic CT reports were searched for the keywords of "Lungenmasse, Masse, Lungenneoplasie, Neoplasie, Lungentumor, Tumor". If any of those keywords were found, the patient information system was searched for the presence of histology of the reported mass. If a lung tumor was confirmed, the patient was included in the study.

To retrieve cases from NC State University several online meetings with the corresponding radiologist and a dedicated research technician were held. To search the patient information system, the PhD student had to pass a security check. This process took approximately one week. After passing the security check, the PhD student got a visiting ID and was asked to install a two-step verifying system in order to access the NC State University systems. An introduction to the patient information system was provided by the corresponding radiologist and through online tutorials. For the most recent cases the PhD student was searching the CT reports via a keyword search of the system. The research technician in cooperation with the local IT was searching the rest of the data base with the keywords and provided the PhD student with a list. The PhD student from this point on was checking those cases for the inclusion criteria in two different platforms. In case of upcoming questions, the PhD student reached out to the research technician, who provided prompt help.

To retrieve cases from Tufts University the host supervisor searched the local data base and provided the PhD student with a list which was checked for the inclusion criteria.

Finally, the thoracic CTs of the included patients were consequently manually downloaded. The CTs from Vetmeduni could be manually anonymized before downloading. For downloading the CTs from NC State University the research technician provided the PhD student with the necessary software. The CTs from Tufts University were provided by the host supervisor. In a next step the CTs were uploaded in a dedicated viewing software used at Vetmeduni (snygo.via, Siemens Healthineers International AG).

Data collection

For each included case the affiliation (VIE, TUF, NC), patient ID, species (dog, cat), breed, sex, age at diagnosis (date of histological diagnosis – date of birth; in years and rounded to whole number), presenting clinical signs, origin of sample for histological diagnosis (surgery/lobectomy, necropsy), histopathological diagnosis, date of CT, date of histopathology, used CT machine, number of post contrast series was noted.

Assessed CT parameters

CT features of the pulmonary mass included: location (left cranial lung lobe, left caudal lung lobe, right cranial lung lobe, right caudal lung lobe, right middle lung lobe, accessory lung lobe; LCRLL, LCDLL, RCRLL, RCDLL, RMLL, ACLL), distribution (central, peripheral, more than 70% of the lung lobe), shape (round, lobulated/irregular, undefined/pneumonic), margination (smooth, spiculated, ground glass (incomplete, complete)), contact to pleura (broad, pleural tag, no contact), dimensions in mm (craniocaudal, laterolateral, dorsoventral). Characteristics of the involved bronchi and vessels were assessed: lobar bronchus terminology, type (normal, displaced, compressed) and segmental bronchus/bronchi terminology, type (periphery, central, displaced), diameter (normal, narrowed, collapsed/obstructed) and luminal surface (smooth, irregular), presence of subsegmental bronchi and air bronchograms, presence of displaced pulmonary vessels by the pulmonary mass, presence of neovascularization. Additionally, the attenuation of the mass was measured in pre- and post-contrast series and graded subjectively as homogeneous, heterogeneous or contrast enhancing rim. The presence of intralesional gas and mineralization (absence, mild, severe), pulmonary nodules (absence, single, multiple), pleural effusion (absence, presence) and features of tracheobronchial lymph nodes (maximum diameter in mm; homogeneous or heterogeneous contrast enhancement) were reported. Bronchial terminology was applied according to de Mello Souza and Reinero (2016, Fig. 1) and Scrivani and Percival (2023, Fig. 2). However instead of cartilaginous bronchus the term subsegmental bronchus was used. There are three observers (CS, SK, AA) and the images are reviewed in consensus.

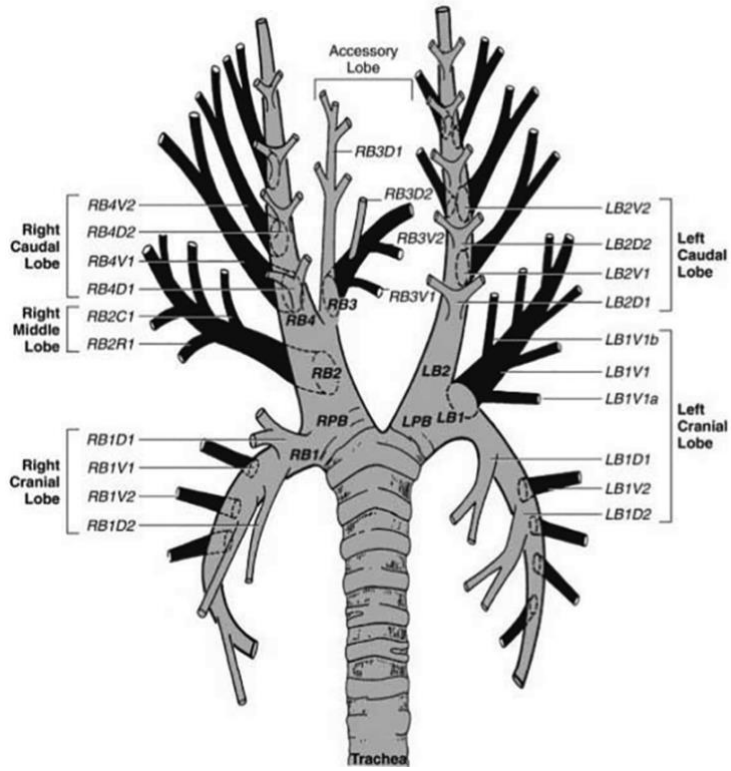

Fig.1. Diagram of the canine bronchial tree (de Mello Souza and Reinero 2016).

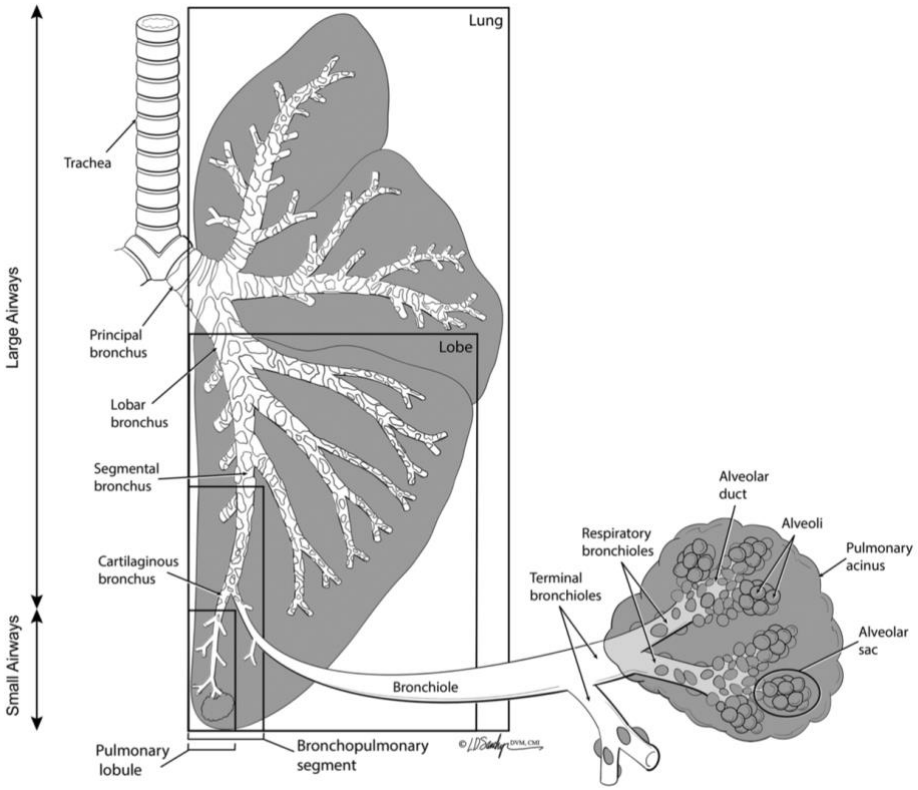

Fig. 2. Illustration relating four lung divisions (boxes) to named bronchial branches (Scrivani and Percival 2023).

5 Results

Based on the inclusion criteria 68 dogs and 21 cats were included.

Dogs: There were 27 male (22 neutered, five intact), 41 female (39 spayed, two intact) dogs. Breeds included Mixed breeds (13), Labrador Retriever (7), Bernese Mountain Dog (4), Standard Poodle (4), Beagle (3), Jack Russel Terrier (3), West-Highland White Terrier (3), Boxer (2), Maltese (2), Rat Terrier (2), Shetland Sheep Dog (2). One dog of each of the following breeds: Golden Retriever, Irish Red and White Setter, Setter, Weimaraner, Magyar Vizsla, German Shepherd, Chow-Chow, Basset, Pit Bull, Golden Doodle, Miniature Schnauzer, Dobermann Pinscher, Airdale Terrier, English Springer Spaniel, Small Münsterländer, Australian Shepherd, Boston Terrier, Havanese, Australian Cattle Dog, English Bulldog, French Bulldog, Shi Tzu, Bichon Frisé.

The age at the time of diagnosis ranged from 2 to 15 years. In 27 cases (chronic) cough was the main presenting complaint. One dog presented in shock, one dog with hemoptysis, two dogs had fever and three dogs with panting/respiratory distress. A pulmonary mass was previously seen on radiographs in eight dogs, and six dogs of those showed prior clinical signs. In 19 dogs a pulmonary mass was diagnosed incidentally.

The origin of the histologic sample was obtained in seven dogs from necropsy and 61 dogs from lobectomy. The histopathological terminology varied between institutions. There were 33 adenocarcinomas (metastasis to lung and lymph nodes (2), lung and bone (1), to the lung alone (3), lymphatic invasion (2), lymph nodes (1)). If a histologic subtype of those was mentioned, the type was papillary (11), papillary-acinar (1), lepidic to papillary (2), papillary-solid (2). 21 lung tumors were classified as carcinomas (metastasis to lung (1), to lung and lymphatic invasion (1), carcinomatosis (1)). There were additionally three adenosquamous carcinomas (metastasis to lung and lymph nodes (1)), seven histiocytic sarcomas (metastasis to lymph nodes (1)), one carcinosarcoma, one sarcoma, one lymphoma and two squamous cell carcinomas.

CT images were acquired with either a 16 or 64 slice CT scanner.

Cats: There were 13 male (castrated) and eight female (spayed) cats. Breeds included Domestic Short Hair (14/21), Domestic Long Hair (3/21), Mixed breed (2/21), Himalayan (1/21), Ragdoll (1/21).

The age at the time of diagnosis ranged from 2 to 16 years. In 10/21 cases respiratory signs have been the presenting complaint (five cases with dyspnea, four case with chronic cough, one case with stridor). Four cats were referred for further work up due to a detected lung mass, one

of them showing additional stridor. In six cats there were no clinical signs and the diagnosis of a pulmonary tumor was incidental. One cat was presented due to vomiting.
The origin of the histologic sample was obtained in seven cases from necropsy and in 14 cases from lobectomy/surgery. The histopathological terminology varied between institutions. There were nine pulmonary carcinomas with one of them showing intra bronchiolar and intravascular invasion and one with intrapulmonary, lymph node, and diaphragmatic metastasis. Seven cases have been diagnosed as an adenocarcinoma with two of them showing metastasis (one case with lymph node metastasis and one with metastasis to the pleura, pericard and diaphragm). One case was classified as bronchoalveolar carcinoma, two cases as adenosquamous carcinoma and two cases as squamous cell carcinoma.
CT images were acquired with either a 16 or 64 slice CT scanner.

Pilot study

After adapting the evaluation criteria, a pilot study of nine dogs of the study population was conducted. Those included three male (one neutered, two intact) and six female (spayed) dogs. Breed included two Setter, two Jack Russel Terrier, and one dog of each of the following breeds German Shepherd, Bernese Mountain Dog, Airedale Terrier and Boxer.
The age at the time of diagnosis ranged from 7 to 15 years. In two cases (chronic) cough was the main presenting complaint. A pulmonary mass was previously seen on radiographs in five dogs, with three dogs of those showing prior clinical signs. In two dogs a pulmonary mass was diagnosed incidentally. The origin of the histologic sample was obtained in all dogs from lobectomy.
There were four adenocarcinomas. If a histologic subtype of those was mentioned, the type was papillary (1), papillary-acinar (1), lepidic to papillary (1), papillary-solid (1). Two lung tumors were classified as carcinomas. There was additionally one adenosquamous carcinoma, one histiocytic sarcoma and one carcinosarcoma.
CT findings
Location of the pulmonary mass
8/9 dogs had a solitary pulmonary mass (left cranial lung lobe (2), left caudal lung lobe (1), right cranial lung lobe (1), right caudal lung lobe (2), right middle lung lobe (0), accessory lung lobe (2)). One dog had a pulmonary mass in the left cranial and left caudal lung lobe respectively.

Distribution of the pulmonary mass in the thorax

Two pulmonary masses were centrally located, while five masses were noted peripherally. Two masses were central as well as peripheral and two masses occupied more than 70% of the lung lobe. Figure 3 shows representative CT images of each type of distribution.

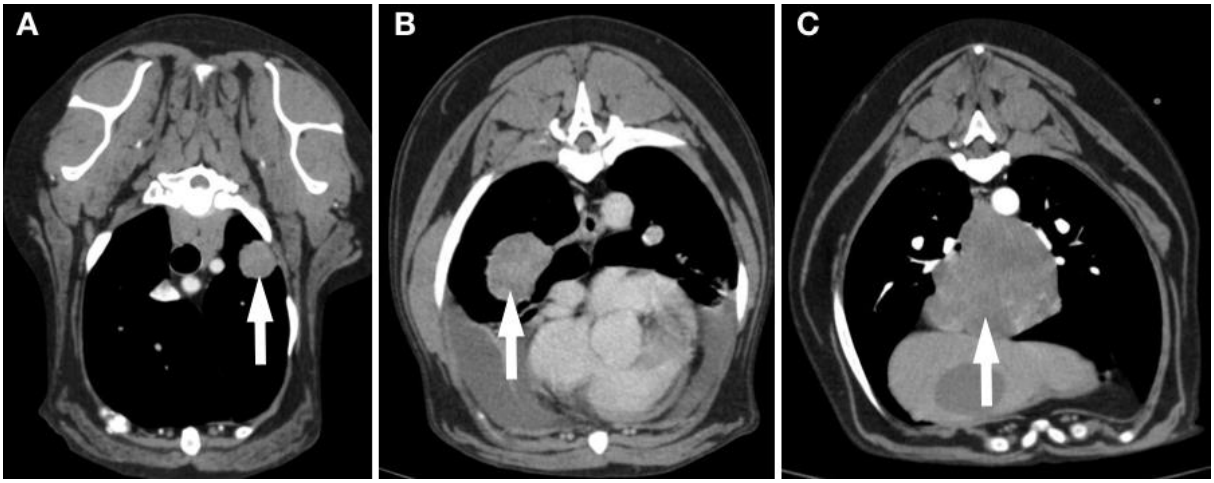

Figure 3. Distribution of lung tumors on transverse post-contrast CT images. A, peripheral (dog 7); B, central (dog 8); C, >70% of lung lobe (dog 1).

Shape of the pulmonary mass

Most of the pulmonary masses showed a round shape (5/9). In two cases each a lobulated/irregular or undefined/pneumonic shape was noted. An example of each type of shape is shown in figure 4.

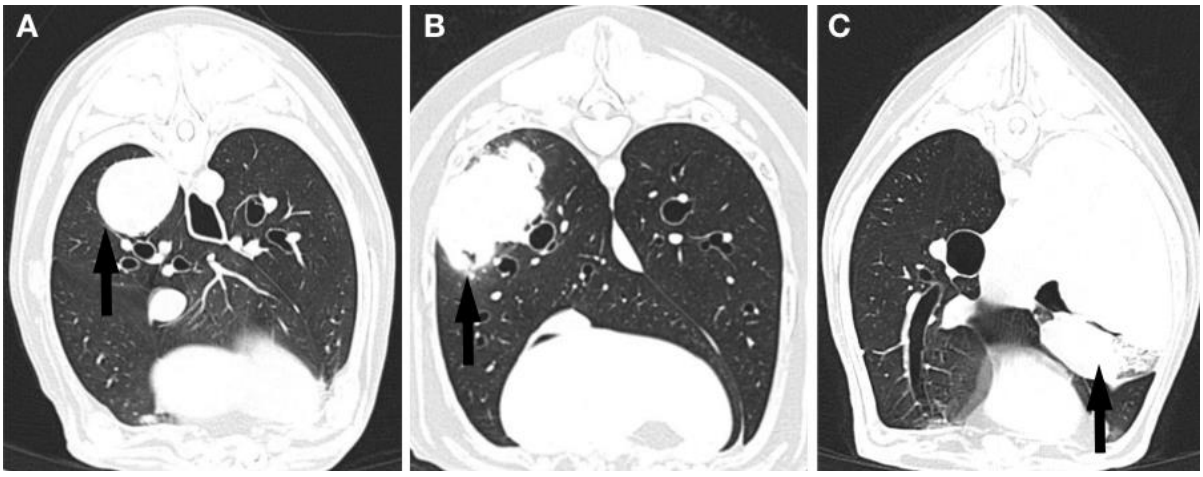

Figure 4. Shape of lung tumors on transverse CT images in lung window. A, round (dog 9); B, lobulated/irregular (dog 2); C, undefined/pneumonic (dog 4).

Margination of the pulmonary mass

The predominant margination was smooth (7/9). In 2/9 cases a spiculated margination was noted and in two cases there was a ground-glass opacity. Figure 5 shows examples of the three different types of margination of pulmonary masses

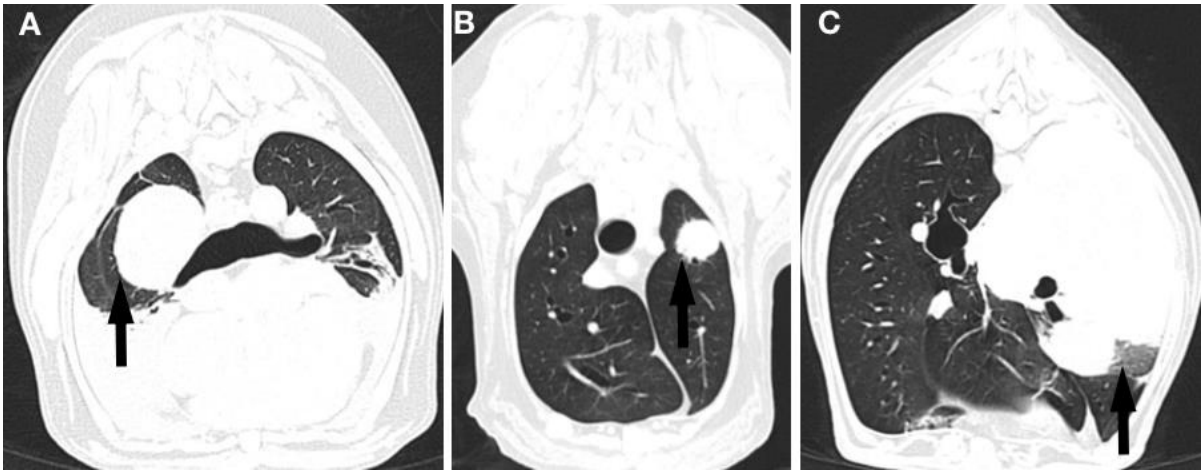

Figure 5. Margin of lung tumors on transverse CT images in lung window. A, smooth (dog 8); B, spiculated (dog 7); C, ground-glass opacity (dog 4).

Contact of the pulmonary mass to the pleura

All pulmonary masses showed a broad contact to the pleura. In two additional cases there were concurrent pleural tags. Figure 6 displays examples of the two different pleura to pulmonary mass contact forms.

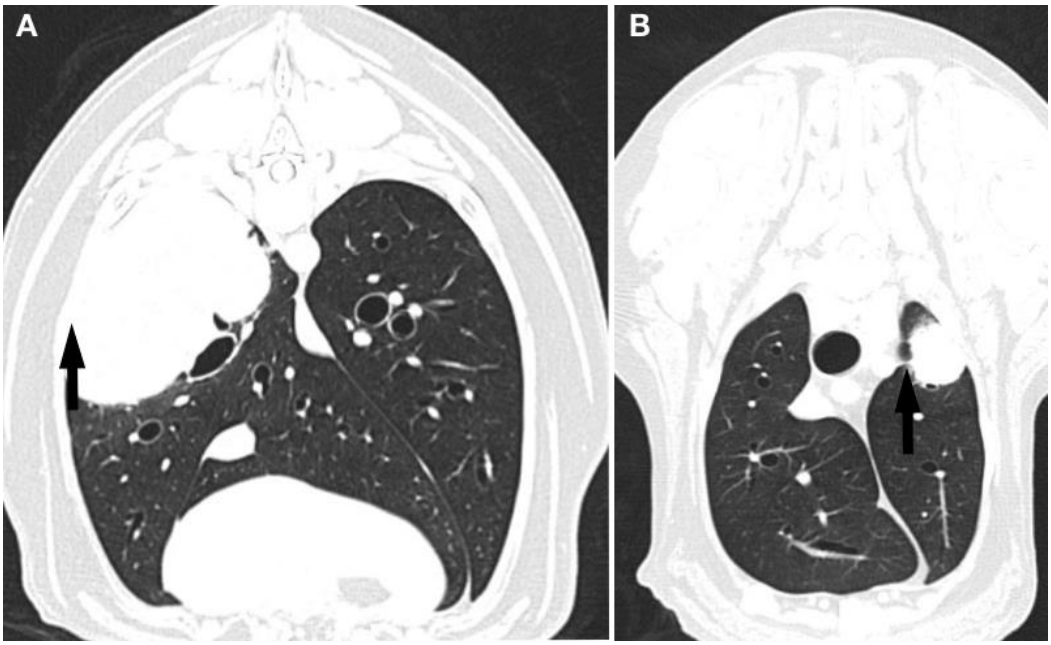

Figure 6. Pleural contact of lung tumors on transverse CT images in lung window. A, broad pleural contact (dog 2); B, pleural tag (dog 7).

The size of the pulmonary mass in millimeter (mm)

The craniocaudal, dorsoventral and laterolateral dimension ranged from 19-76 mm, 11-87 mm and 21-87 mm respectively.

Lobar bronchus type

A lobar bronchus was most commonly (8/9) affected by the pulmonary mass in terms of being displaced and compressed (Table 1, Figure 7).

	Lobar bronchus
Dog 1	D,C
Dog 2	D,C
Dog 3	D,C
Dog 4	D,C
Dog 5	D,C
Dog 6	D,C
Dog 7	N
Dog 8	D,C
Dog 9	D,C

Table 1. Lobar bronchus type. N, normal; D, displaced; C, compressed.

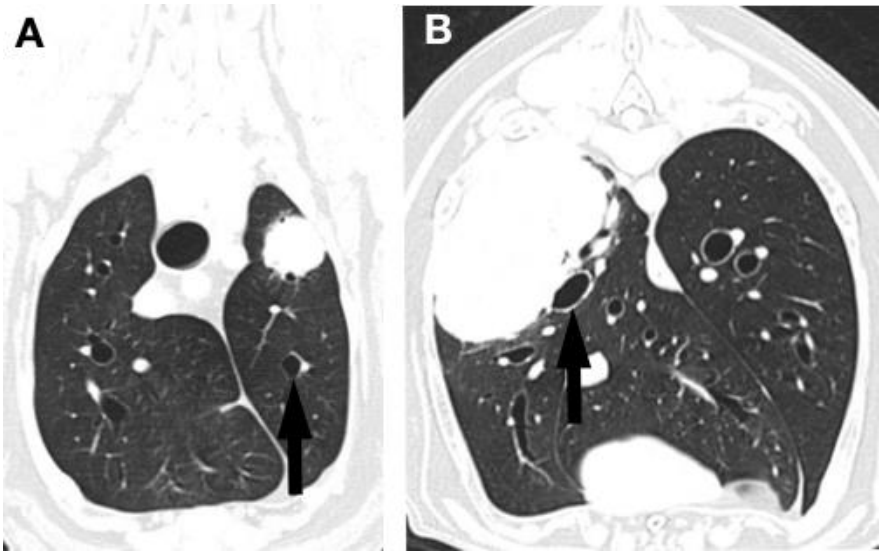

Figure 7. Lobar bronchus type on transverse CT images in lung window. A, normal (dog 7); B, displaced and compressed (dog 2).

Segmental bronchus

One segmental bronchus was affected by the pulmonary mass in all cases and two bronchi in six cases. A third, fourth and fifth segmental bronchus was affected in three, one and one cases respectively.

Location of segmental bronchus

Most commonly, namely 12 out 20 altered segmental bronchi were peripheral located within the pulmonary mass and displaced at the same time (Table 2, Figure 8).

	Segmental bronchus 1	**Segmental bronchus 2**	**Segmental bronchus 3**	**Segmental bronchus 4**	**Segmental bronchus 5**
Dog 1	C	P	-	-	-
Dog 2	P, D	C	P, D	-	-
Dog 3	P, D	P, D	-	-	-
Dog 4	P	P	C	P, D	P, D
Dog 5	P	-	-	-	-
Dog 6	P, D	-	-	-	-
Dog 7	P, D	-	-	-	-
Dog 8	P, D	P, D	-	-	-
Dog 9	P, D	P, D	D	-	-

Table 2. Location of segmental bronchus. C, central; P, peripheral; D, displaced.

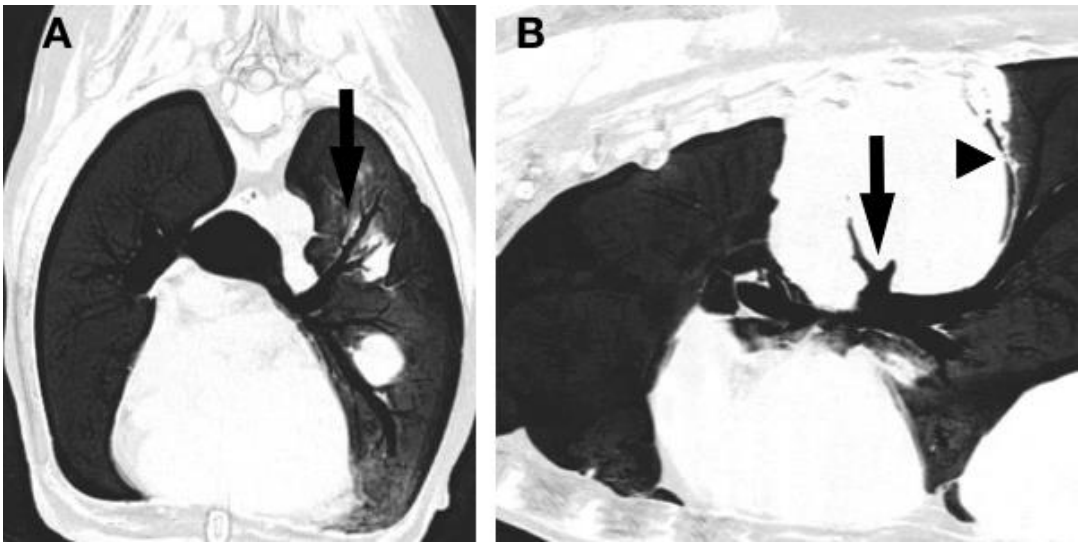

Figure 8. Location of segmental bronchus associated with lung tumors. Minimum intensity projection images (A, transverse image; B, sagittal reformatted image) of dog 4. A, peripheral located segmental bronchus; B, central (black arrow), peripheral and displaced (black arrowhead) segmental bronchi associated with a lung tumor.

Diameter of segmental bronchus

The diameter of affected segmental bronchi were normal, narrowed or collapsed in three, 11 or six out of 20 bronchi (Table 3, Figure 9).

	Segmental bronchus 1	**Segmental bronchus 2**	**Segmental bronchus 3**	**Segmental bronchus 4**	**Segmental bronchus 5**
Dog 1	NW	NW	-	-	-
Dog 2	NO	CO	NW	-	-
Dog 3	NW	NW	-	-	-
Dog 4	NO	NO	CO	CO	NW
Dog 5	CO	-	-	-	-
Dog 6	NW	-	-	-	-
Dog 7	NW	-	-	-	-
Dog 8	NW	NW	-	-	-
Dog 9	CO	CO	NW	-	-

Table 3. Diameter of segmental bronchus. NO, normal; NW, narrowed; CO, collapsed/obstruction.

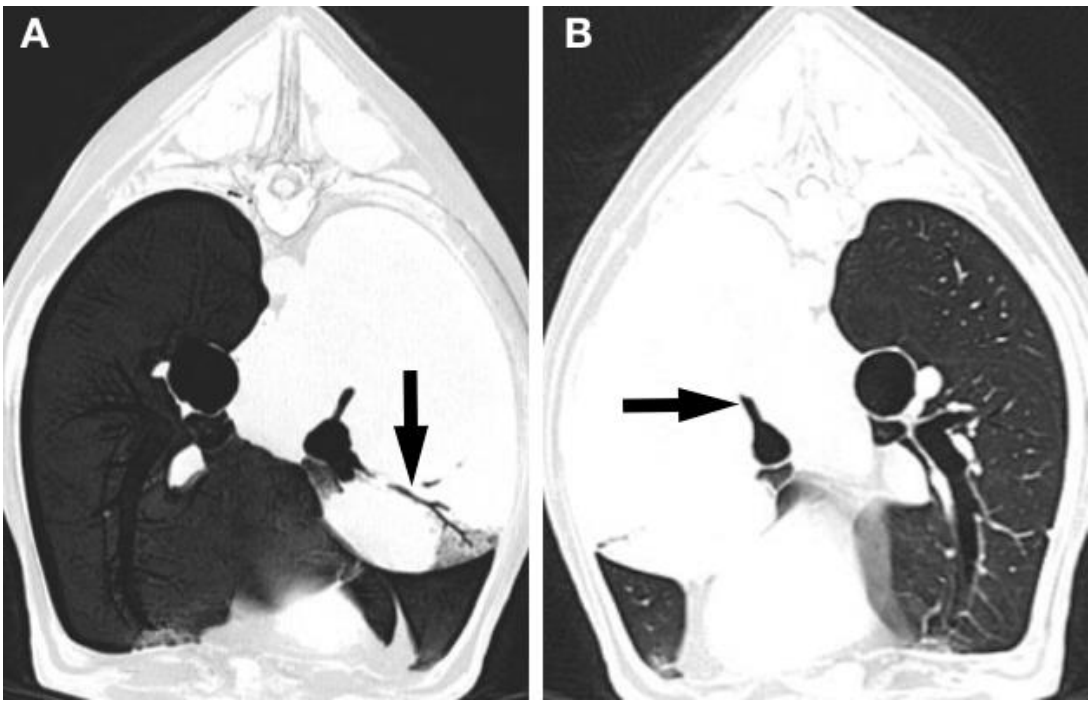

Figure 9. Diameter of segmental bronchi associated with lung tumors. Transverse images (A, minimum intensity projection; B, lung window) showing a narrowed (A) and collapsed/obstructed (B) segmental bronchus of dog 4.

Luminal surface of the segmental bronchus

The inner surface of affected bronchi was considered smooth in 18 cases while in two cases the surface was considered irregular (Table 4, Figure 10).

	Segmental bronchus 1	**Segmental bronchus 2**	**Segmental bronchus 3**	**Segmental bronchus 4**	**Segmental bronchus 5**
Dog 1	S	S	-	-	-
Dog 2	S	S	S	-	-
Dog 3	I	I	-	-	-
Dog 4	S	S	S	S	S
Dog 5	S	-	-	-	-
Dog 6	S	-	-	-	-
Dog 7	S	-	-	-	-
Dog 8	S	S	-	-	-
Dog 9	S	S	S	-	-

Table 4. Luminal surface of the segmental bronchus. S, smooth; I, irregular.

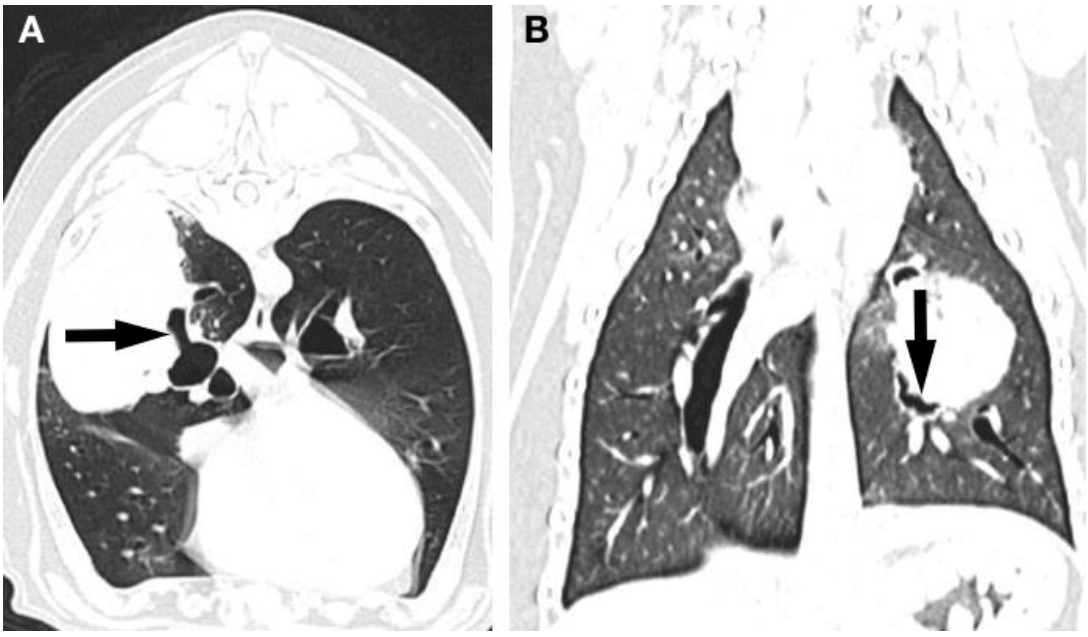

Figure 10. Luminal surface of segmental bronchi affected by lung tumors. A, transverse image in lung window showing a smooth luminal surface of the segmental bronchus (dog 2); B, dorsal reformatted image in lung window showing an irregular luminal surface of a segmental bronchus (dog 3).

Air bronchogram

2/9 pulmonary masses showed an air bronchogram.

Presence of subsegmental bronchi

In four pulmonary masses subsegmental bronchi were seen.

Vascular changes

Displacement of pulmonary vessels by the pulmonary mass was seen in 6/9 cases (Figure 11, A) and neovascularization was noted in 8/9 cases (Figure 11, B).

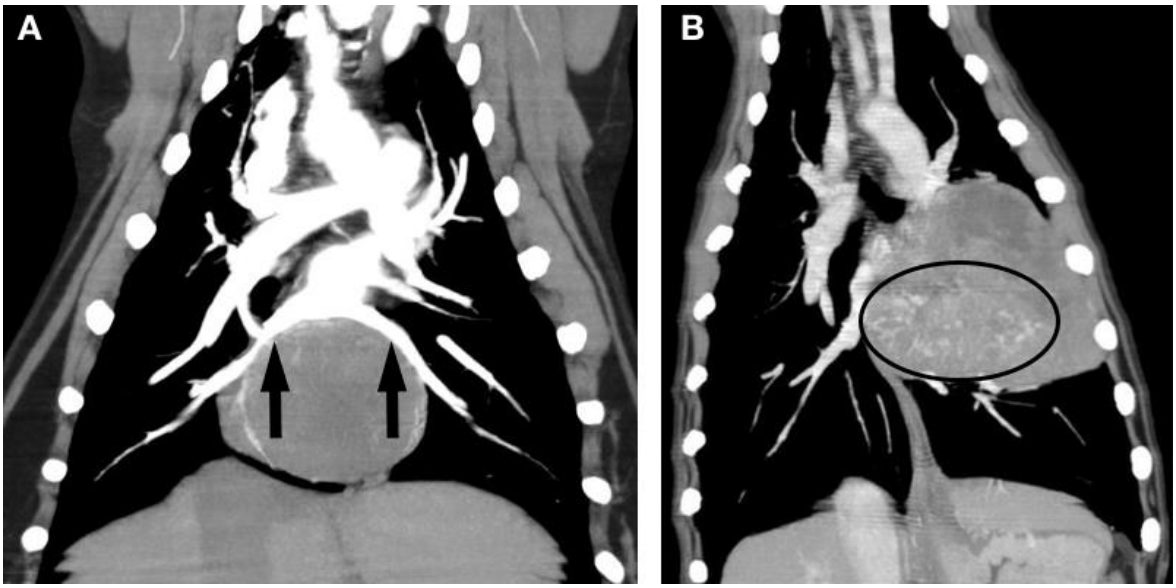

Figure 11. Vascular changes associated with the lung tumors on dorsal reformatted CT images after contrast medium application. A, peripheral displacement of the pulmonary vessels by the pulmonary mass (dog 1); B, additional small branching vessels (neovascularization) are noted (dog 4).

Attenuation

The pre-contrast attenuation ranged between 33 and 55 HU (Hounsfield Unit). There were two, three and four contrast series in six, two and one cases.

The attenuation of the pulmonary mass in the first, second, third and fourth series ranged from 37-77 HU, 49-79 HU, 44-77 HU and 63 HU respectively.

In 6/9 cases a heterogeneous contrast enhancement was noted. An incomplete contrast enhancing rim was suggested in 7/9 cases.

Intralesional gas, mineralization

No intralesional gas was seen in any pulmonary mass. 4/9 pulmonary masses showed mild mineralization, while one mass showed severe amount of mineralization.

Additional findings

One dog each had multiple pulmonary nodules and pleural effusion.

Tracheobronchial lymph nodes

The maximum dimension of a tracheobronchial lymph node size ranged from 5-12 mm. The post-contrast appearance was homogeneous in eight cases and heterogeneous in one case.

6 Discussion

Challenges/Mitigating circumstances

Challenges of a multicenter study were various and heightened by COVID-19 mitigating circumstances.

With increasing number of collaborators also the number of challenges increase, including personal and technical challenges. Firstly, periods of illnesses need to be considered, yet this cannot be predicted. The PhD student suffered from COVID-19 shortly before the start of the project and one observer during the project. Unfortunately, another collaborator suffered from an illness requiring surgery and above that was subjected to visa issues compromising availability. Moreover, planning online meetings with collaborators of different time zones is challenging and needs to be considered to add additional time in case of technical obstacles on different ends, which happened in a few meetings.

Apart from that, the authors spent two months reviewing cases and adapting the evaluation criteria. First, a human grading system for bronchial and vascular changes according to Wang et al. (2011) was anticipated. The authors in that study used four evaluation criteria namely: (1) an obstruction abruptly at the edge of a nodule; (2) a tapered interruption at the center of nodule; (3) penetrating through the nodule; or (4) contacting the nodule but stretched or encased.

However, the observers of the current study experienced common problems in applying this grading system as it was considered challenging to agree on those criteria implying multiple features at the same time (eg. obstruction at the edge, interruption at the center). Since in human medicine lung tumors are usually diagnosed at a much earlier state in comparison to domestic animals, lung tumors in domestic animals are usually much bigger at the time of diagnosis. Thus, the involved bronchovascular structures might be more altered and show a bigger range of features in bigger tumors. Additionally, in bigger masses the anatomical identification of bronchovascular structures might be distorted, making an accurate identification challenging. As a result, the authors decided to adapt the evaluation criteria by assessing the location of the lobar, segmental and subsegmental bronchi in respect to the pulmonary mass, as well as the diameter and the luminal surface of those structures. The assessment of vascular structures was even more simplified by only assessing signs of mass effect on the vessels or the presence of neovascularization. Concerning post-processing tool, multiplanar reconstruction and minimal intensity projection images (MINIP) were used to assess the involved bronchus or bronchi. A MINIP is a post-processing reconstruction used by the software to highlight structures of similar low attenuation, namely gas in the conducting airways (bronchi), facilitating the visualization

of branching and identification of bronchi. Besides that, the authors agreed to conduct the study evaluating the imaging criteria in consensus.

Discussion of CT features in general

In this project the authors retrieved data of 68 dogs and 21 cats and conducted a pilot study in nine dogs of the study population. As a consequence of this pilot study an evaluation of the entire study population will follow.

Overall, diagnostic imaging publications on CT features of lung tumors in dogs and cats are sparse (Marolf et al. 2011, Tsai et al. 2012, Aarvold et al. 2015, Parry et al. 2021, Bello et al. 2021) and include general imaging features to date. Especially advanced imaging features of lung tumors as used in human medicine are lacking in veterinary medicine. As CT has a critical role in diagnosing, staging, surgical-planning and monitoring patients with lung tumors, scientific imaging articles in humans focus on identifying CT criteria that can be prognostically useful and help elucidating the pathogenesis of lung tumors. Human articles mainly focus therefore on bronchovascular changes, pathologic-radiologic correlation, lung mass morphology and advanced modalities. Similar to the literature and the findings of the current study, the most common lung tumor is the adenocarcinoma in dogs and cats. Since also in humans the adenocarcinoma is the most common lung tumor, also a large number of articles in human medicine focus on this tumor type. However, the terminology in humans is different since lung tumors are divided into small-cell lung carcinoma (SCLC) and non-small-cell lung carcinoma (NSCLC). The majority (85%) of lung tumors are nonetheless NSCLC, with adenocarcinomas being the most common type (Wang et al. 2022).

<u>Bronchovascular changes associated with lung tumors</u>

In this pilot study we found lung tumors involving at least one segmental bronchus in all cases. The involvement of multiple segmental bronchi might be attributed consequently by the larger size of the pulmonary mass. Thus, the evaluation of segmental bronchi warrants further evaluation in the entire study population. An affection of the subsegmental bronchi were difficult to evaluate. Since they are third order bronchi they are very small and thought to be easier obscured by the tumor thus hindering the detection.

The relationship of pulmonary masses with the corresponding bronchi and vessels has been studied intensively in human medicine. In a study from Wang et al. (2011) the authors described pulmonary artery, pulmonary vein and the associated bronchus in the relation to peripheral lung tumors as either abruptly obstructed at the edge of the tumor, tapered interruption at the center of the tumor, penetrating through the tumor or in contact with the tumor but stretched or

encased. They reported that the vast majority of the bronchi and pulmonary artery were interrupted by the tumor. Regarding bronchi and pulmonary arteries, an abruptly obstructed pattern was seen more often with solid, larger than 2 cm nodules and a tapered interruption at the center of the tumor was seen in part-solid, non-solid lesions. Regarding the pulmonary vein, a tapered interruption was seen at the center of the tumor, that were part-solid and non-solid. A malignant behavior of pulmonary arterial encasement was further demonstrated by Lin et al. (2015) as the authors showed that the average degrees of pulmonary arterial encasement were higher in malignant than in benign masses.

Besides of those interesting findings it important to consider the spatial resolution for the detection of small, branching structure such as vessels and bronchi. It is reported that the blood supply of most lung tumors is coming from bronchial arteries (Lin et al. 2015). Generally, the lungs are characterized by a dual vascular supply namely by pulmonary and bronchial vessels. While the pulmonary arteries' role is gas exchange, the bronchial arteries' goal is to support bronchial tree, large blood vessels, lymph nodes, esophagus, and pleura with oxygenated blood. Bronchial arteries are much smaller than pulmonary arteries and difficult to detect on CT if no dilation is present (Almeida et al. 2020). For example, in a 2-4 cm mass the biggest lumen of the feeding bronchial artery is said to be between 200 and 600 μm. Since the minimal thickness of 16-slice CT is 0.625 mm, in lesions that are smaller than 4 cm the spatial resolution might not be sufficient to be display bronchial arterial supply. Besides that, a pulmonary artery associated with a peripheral lung lesion can be detected if it was seen up to 2 cm to the pleura. In general the blood supply of lung tumors changes with the size of the tumor. It is said that at an early stage of the tumor growth the bronchial arteries show a hilifugal pattern, while in more advanced stages they build a wool ball-like pattern. Tumors bigger than 4-6 cm will further show necrotic central areas and more vascularization in the periphery of the tumor comprising bronchial artery-to-pulmonary artery anastomoses (Lin et al. 2015).

In a very recent prospective anatomic study examining the canine lower airway lumen morphology, the authors describe identification to the cartilaginous bronchi (which are called subsegmental in the current study) with CT of the normal lung (Scrivani and Percival 2023).

Lung mass morphology

Although different general morphologic findings were seen in the pilot study a statistical analysis of the larger study population is warranted.

In humans so far, several features have been shown to be prognostically helpful. Spiculation, which is also called sunburst or corona radiata sign, is related to interlobular septal thickening, obstruction of pulmonary vessels or lymphatic channels filled with tumor cells. Cavitation is

thought to be due to necrosis of the central aspect of the mass and is predominantly described in squamous cell carcinoma and metastasis. A cystic airspace in contact with a pulmonary nodule is indicative of malignancy, with adenocarcinoma being the most common tumor type. Suggested pathogenesis includes a check-valve mechanism involving the small airways and neoplastic growth along the wall of a preexisting bulla (Snoeckx et al. 2018).

Since the size of a lung mass and the monitoring of its growth has an impact on patient staging, Han et al. (2018) assessed the influence of the lung mass margin on inter- and intra-observer variability in diameter measurements in comparison to semi-automatic volume measurements. The authors showed a larger inter-observer variability for manual diameter measurement results leading to an inaccurate lung nodule growth detection and size classification (Han et al. 2018).

Radiologic-pathologic correlation

Since ground-glass opacities and pleural tags were also findings in the current pilot study, those findings will be of specific interest to evaluate in the entire study population. Those features have been described in human medicine correlated to pathologic findings. An interdisciplinary approach in cancer management by means of correlation of radiologic and pathologic findings helps to better understand the pathogenesis of lung tumors and to improve the impact of certain imaging features. Evaluating the CT attenuation of lung tumors and their size have been shown to be important prognostic features, since even small ground-glass nodules less than 1 cm have even been described as malignant lesions (Xiang et al. 2014). Ground glass is defined in CT as an area of hazy increased attenuation of the lung that does not obscure underlying bronchial structures or pulmonary vessels (Gao et al. 2017). Xiang et al. (2014) reported that ground-glass nodules from 6.5 mm to 10 mm with a well-defined and coarse interface could indicate adenocarcinoma in situ or minimally invasive adenocarcinoma. Regarding the prognosis, a strong association between the percentage of ground-glass opacity of the tumor and lepidic growth, which carries a better prognosis than other histological grades, was found (Lederlin et al. 2013). This highlights the potential importance of studies on radiologic-pathologic correlation in terms of tumor subtyping and as prognostic puzzle pieces.

In a further radiologic-pathologic comparison Ambrosi et al. (2020) demonstrated that the solid part of a tumor besides resulting from infiltration can also be caused by tumor atelectasis. A proposed explanation of tumor atelectasis is an increased stiffness of alveolar walls due to tumor cells. As a consequence of this stiffness, there is a higher resistance during inspiration which results in less air flow in the tumor (Ambrosi et al. 2020).

Another type of infiltration has been described regarding the pleura. In human medicine pleural infiltration associated with lung tumors has been shown to have an important prognostic impact

as the five-year survival rate decreased from 86% to 62-70% in case of visceral pleural infiltration (Oyama et al. 2013). Hsu et al. (2016) showed an increase accuracy of early diagnosis of NSCLC with visceral pleural infiltration by detecting type 2 pleural tags on CT images. A pleural tag is described as a linear structure which extends from the surface of a peripheral lung mass to the pleural surface due to thickening of interlobular septa of the lung. From pleural tag type 1 to 3 the connection between the surface of the lung tumor and the pleura increases in thickness. While in type 1 a linear strand can be only seen in a lung window, in type 2 this connection gets thicker and is evident on a soft-tissue window (Hsu et al. 2016).

On an even more advanced level, the increasing use of artificial intelligence in human medicine with the big benefit to process large amount of complex radiologic-pathologic information plays a vital role in the medical field. Historically diagnosis of lung tumors is achieved through histological evaluation in veterinary and human medicine. However, histologic examination of individual samples of lung tumors are biased by the specific location from where they are retrieved within the tumor. Unfortunately, it has been shown in human medicine that lung tumors show heterogeneous features regarding genetic and phenotypic characteristics throughout the tumor (Jamal-Hanjani et al. 2017). As technology is continuously advancing, new emerging non-invasive imaging analysis called radiomics are evolving that add to the physician's descriptive report. Texture analysis is one of those tools using highly computerized algorithms that retrieve high magnitude of data from CT images on complex levels. With this analysis on the one hand a histogram comprising image features is created. Those characteristics have been shown to reflect various histopathological parameters of tumors. On the other hand, this analysis can display the spatial relationship of neighboring gray levels of voxels thus demonstrating the intralesional heterogeneity of a tumor (Incoronato et al. 2017, El Ayachy et al. 2021). These information can be further used for the development of future imaging biomarkers, which could be used to improve cancer patient management. One valuable applicability might lie in correlating those data with molecular alterations in terms of prognosis and treatment of pulmonary adenocarcinoma. Patients with epidermal growth factor receptor (EGFR) mutations have shown an increased response to chemotherapy in comparison to those without the EGFR mutations. Interestingly, several radiomic features seem to be associated with EGFR mutation statuses of lung adenocarcinoma in humans making it potentially useful for future medical management (Mai et al. 2018). In veterinary medicine articles about machine learning-based approaches have increased in general in the last years, yet articles specifically on lung tumors are lacking (Burti et al. 2022, Schmid et al. 2022).

7 Conclusion/Future prospects

Lung tumors in dogs and cats mainly occur in middle-aged to old patients and will be of increasing veterinary interest since domestic animals are progressively getting older similar to their human counterparts. For a successful treatment, an accurate diagnostic workup is crucial for refinement of prognosis and ultimately improved therapeutical approaches. Up to date only basic descriptive diagnostic imaging features of lung tumors in dogs and cats have been published. Likewise to human medicine the aim of the current project is to further assess more in depth CT features of lung tumor which might contribute to the understanding of the pathogenesis of this disease and decision-making for a dedicated treatment. In future similar to human medicine better classification of lung tumor types and correlation of specific CT features with pathology, in particular with the help of advancement in imaging techniques such as texture analysis and machine-based learning, might additionally pave the way for further therapeutic and diagnostic approaches. Based on an increasing knowledge also other therapeutic strategies such a personalized treatment associated with molecular alterations as in human medicine might also gain increasing importance.

In conclusion, due to consideration of mitigating circumstances leading to remote research with technical and collaborating challenges, after performing the pilot study the next step is assessing the rest of the study population with the established evaluation criteria and perform a statistical analysis. With the partial and future results of our project, the authors want to contribute to the understanding of lung tumors in veterinary medicine and hope to pave the way for further studies similar to human medicine.

8 References

Aarsvold S, Reetz JA, Reichle JK, Jones ID, Lamb CR, Evola MG, et al. Computed tomographic findings in 57 cats with primary pulmonary neoplasia. Vet Radiol Ultrasound. 2015;56(3):272-7. doi: 10.1111/vru.12240.

Almeida J, Leal C, Figueiredo L. Evaluation of the bronchial arteries: normal findings, hypertrophy and embolization in patients with hemoptysis. Insights Imaging. 2020;11(1):70. doi: 10.1186/s13244-020-00877-4.

Ambrosi F, Lissenberg-Witte B, Comans E, Sprengers R, Dickhoff C, Bahce I, et al. Tumor Atelectasis Gives Rise to a Solid Appearance in Pulmonary Adenocarcinomas on High-Resolution Computed Tomography. JTO Clin Res Rep. 2020;1(2):100018. doi: 10.1016/j.jtocrr.2020.100018.

Ballegeer EA, Adams WM, Dubielzig RR, Paoloni MC, Klauer JM, Keuler NS. Computed tomography characteristics of canine tracheobronchial lymph node metastasis. Vet Radiol Ultrasound. 2010;51(4):397-403. doi: 10.1111/j.1740-8261.2010.01675.x.

Bello AM, Anselmi C, Frau M, Berman KG, Novellas R, Espada Y, et al. Pulmonary carcinoma associated with cystic airspaces in two dogs. J Small Anim Pract. 2022;63(6):486-491. doi: 10.1111/jsap.13451.

Burti S, Zotti A, Bonsembiante F, Contiero B, Banzato T. A Machine Learning-Based Approach for Classification of Focal Splenic Lesions Based on Their CT Features. Front Vet Sci. 2022;9:872618. doi: 10.3389/fvets.2022.872618.

Cetinkaya MA, Yardimci B, Yardimci C. Hypertrophic osteopathy in a dog associated with intra-thoracic lesions: A case report and a review. Veterinární medicína. 2011;56:595-601. 10.17221/4437-VETMED.

Cozzi B, Ballarin C, Mantovani R, Rota A. Aging and Veterinary Care of Cats, Dogs, and Horses through the Records of Three University Veterinary Hospitals. Front Vet Sci. 2017;4:14. doi: 10.3389/fvets.2017.00014.

Culp WTN, Rebhun RB. Tumors of the Respiratory System. In: Withrow and MacEwen's Small Animal Clinical Oncology. Sixth edition. Editors: Vail DM, Thamm DH, Liptak JM. Elsevier, St. Louis, Missouri, 2020a. p.511-512.

Culp WTN, Rebhun RB. Tumors of the Respiratory System. In: Withrow and MacEwen's Small Animal Clinical Oncology. Sixth edition. Editors: Vail DM, Thamm DH, Liptak JM. Elsevier, St. Louis, Missouri, 2020b. p.507.

De Mello Souza CH, Reinero CR. Effects of successive tracheal resection and anastomosis on tracheal diameter and position of lobar bronchi in dogs. Am J Vet Res. 2016;77(6):658-63. doi: 10.2460/ajvr.77.6.658.

Dobson JM, Samuel S, Milstein H, Rogers K, Wood JL. Canine neoplasia in the UK: estimates of incidence rates from a population of insured dogs. J Small Anim Pract. 2002;43:240–246. doi: 10.1111/j.1748-5827.2002.tb00066.x.

D'Costa S, Yoon BI, Kim DY, Motsinger-Reif AA, Williams M, Kim Y. Morphologic and molecular analysis of 39 spontaneous feline pulmonary carcinomas. Vet Pathol. 2012;49:971–978. doi: 10.1177/0300985811419529.

El Ayachy R, Giraud N, Giraud P, Durdux C, Giraud P, Burgun A, et al. The Role of Radiomics in Lung Cancer: From Screening to Treatment and Follow-Up. Front Oncol. 2021 May 5;11:603595. doi: 10.3389/fonc.2021.603595.

Gao JW, Rizzo S, Ma LH, Qiu XY, Warth A, Seki N, et al.; written on behalf of the AME Lung Cancer Collaborative Group. Pulmonary ground-glass opacity: computed tomography features, histopathology and molecular pathology. Translational Lung Cancer Research. 2017;6(1):68-75. doi:10.21037/tlcr.2017.01.02.

Geyer NE, Reichle JK, Valdés-Martínez A, Williams J, Goggin JM, Leach L, et al. Radiographic appearance of confirmed pulmonary lymphoma in cats and dogs. Vet Radiol Ultrasound. 2010;51(4):386-90. doi: 10.1111/j.1740-8261.2010.01683.x.

Goldfinch N, Argyle DJ. Feline lung-digit syndrome: unusual metastatic patterns of primary lung tumours in cats. J Feline Med Surg. 2012;14(3):202-8. doi: 10.1177/1098612X12439267.

Han D, Heuvelmans MA, Vliegenthart R, Rook M, Dorrius MD, de Jonge GJ, et al. Influence of lung nodule margin on volume- and diameter-based reader variability in CT lung cancer screening. Br J Radiol. 2018;91(1090):20170405. doi: 10.1259/bjr.20170405.

Hsu JS, Han IT, Tsai TH, Lin SF, Jaw TS, Liu GC, et al. Pleural Tags on CT Scans to Predict Visceral Pleural Invasion of Non-Small Cell Lung Cancer That Does Not Abut the Pleura. Radiology. 2016;279(2):590-6. doi: 10.1148/radiol.2015151120.

Incoronato M, Aiello M, Infante T, Cavaliere C, Grimaldi AM, Mirabelli P, et al. Radiogenomic Analysis of Oncological Data: A Technical Survey. International Journal of Molecular Sciences. 2017; 18(4):805. https://doi.org/10.3390/ijms18040805.

Jamal-Hanjani M, Wilson GA, McGranahan N, Birkbak NJ, Watkins TBK, Veeriah S, et al. Tracking the Evolution of Non-Small-Cell Lung Cancer. N Engl J Med. 2017 Jun 1;376(22):2109-2121. doi: 10.1056/NEJMoa1616288.

Lederlin M, Puderbach M, Muley T, Schnabel PA, Stenzinger A, Kauczor HU, et al. Correlation of radio- and histomorphological pattern of pulmonary adenocarcinoma. Eur Respir J. 2013;41(4):943-51. doi: 10.1183/09031936.00056612.

Leite-Filho RV, Panziera W, Bandinelli MB, Pavarini SP. Pathological Characterization of Lymphoma with Pulmonary Involvement in Cats. J Comp Pathol. 2018;165:6-12. doi: 10.1016/j.jcpa.2018.09.007.

Lin CH, Li TC, Tsai PP, Lin WC. The relationships of the pulmonary arteries to lung lesions aid in differential diagnosis using computed tomography. Biomedicine (Taipei). 2015;5(2):11. doi: 10.7603/s40681-015-0011-z.

Mei D, Luo Y, Wang Y, Gong J. CT texture analysis of lung adenocarcinoma: can Radiomic features be surrogate biomarkers for EGFR mutation statuses. Cancer Imaging. 2018;18(1):52. doi: 10.1186/s40644-018-0184-2.

Marolf AJ, Gibbons DS, Podell BK, Park RD. Computed tomographic appearance of primary lung tumors in dogs. Vet Radiol Ultrasound. 2011;52(2):168-72. doi: 10.1111/j.1740-8261.2010.01759.x.

McPhetridge JB, Scharf VF, Regier PJ, Toth D, Lorange M, Tremolada G, et al. Distribution of histopathologic types of primary pulmonary neoplasia in dogs and outcome of affected dogs: 340 cases (2010-2019). J Am Vet Med Assoc. 2021;260(2):234-243. doi: 10.2460/javma.20.12.0698.

McNiel EA, Ogilvie GK, Powers BE, Hutchison JM, Salman MD, Withrow SJ. Evaluation of prognostic factors for dogs with primary lung tumors: 67 cases (1985-1992). J Am Vet Med Assoc. 1997;211: 1422-1427.

Moore PF. Canine and Feline Histiocytic Diseases. In: Meuten DJ, editor. Tumors in Domestic Animals. Fifth ed. Iowa, USA: John Wiley & Sons, Inc.; 2017a. p. 325.

Moore PF. Canine and Feline Histiocytic Diseases. In: Meuten DJ, editor. Tumors in Domestic Animals. Fifth ed. Iowa, USA: John Wiley & Sons, Inc.; 2017b. p. 327.

Murray CA, Willcox JL, De Mello Souza CH, Husbands B, Cook MR, Clifford C et al. Outcome in dogs with curative-intent treatment of localized primary pulmonary histiocytic sarcoma. Vet Comp Oncol. 2022;20(2):458-464. doi: 10.1111/vco.12791.

Ogilvie GK, Weigel RM, Haschek WM, Withrow SJ, Richardson RC, Harvey HJ, et al. Prognostic factors for tumor remission and survival in dogs after surgery for primary lung tumor: 76 cases (1975-1985). J Am Vet Med Assoc. 1989;195:109-112.

Oyama M, Miyagi Maeshima A, Tochigi N, Tsuta K, Kawachi R, Sakurai H, et al. Prognostic impact of pleural invasion in 1488 patients with surgically resected non-small cell lung carcinoma. Jpn J Clin Oncol. 2013;43(5):540-6. doi: 10.1093/jjco/hyt039.

Parry M, Selmic LE, Lumbrezer-Johnson S, Lapsley J, Wavreille VA, Hostnik E. Computed tomographic characteristics of cavitary pulmonary adenocarcinoma in 3 dogs and 2 cats. Can Vet J. 2021;62(7):719-724.

Polton G, Finotello R, Sabattini S, Rossi F, Laganga P, Vasconi ME, et al. Survival analysis of dogs with advanced primary lung carcinoma treated by metronomic cyclophosphamide, piroxicam and thalidomide. Vet Comp Oncol. 2018;16:399–408. https://doi.org/10.1111/vco.12393.

Rose RJ, Worley DR. A Contemporary Retrospective Study of Survival in Dogs With Primary Lung Tumors: 40 Cases (2005–2017). Front. Vet. Sci. 2020, 7:519703. doi: 10.3389/fvets.2020.519703.

Santos IR, Raiter J, Lamego ÉC, Bandinelli MB, Dal Pont TP, Siqueira KF, et al. Feline pulmonary carcinoma: Gross, histological, metastatic, and immunohistochemical aspects. Vet Pathol. 2022; 3009858221122517. doi: 10.1177/03009858221122517.

Schmid D, Scholz VB, Kircher PR, Lautenschlaeger IE. Employing deep convolutional neural networks for segmenting the medial retropharyngeal lymph nodes in CT studies of dogs. Vet Radiol Ultrasound. 2022;63(6):763-770. doi: 10.1111/vru.13132.

Scrivani PV, Percival A. Anatomic study of the canine bronchial tree using silicone casts, radiography, and CT. Vet Radiol Ultrasound. 2023;64:36–41. https://doi.org/10.1111/vru.13141.

Smith AJ, Sutton DR, Major AC. CT appearance of presumptively normal intrathoracic lymph nodes in cats. J Feline Med Surg. 2020;22(10):875-881. doi: 10.1177/1098612X19886672.

Snoeckx A, Reyntiens P, Desbuquoit D, Spinhoven MJ, Van Schil PE, van Meerbeeck JP, et al. Evaluation of the solitary pulmonary nodule: size matters, but do not ignore the power of morphology. Insights Imaging. 2018;9(1):73-86. doi: 10.1007/s13244-017-0581-2.

Tsai S, Sutherland-Smith J, Burgess K, Ruthazer R, Sato A. Imaging characteristics of intrathoracic histiocytic sarcoma in dogs. Vet Radiol Ultrasound. 2012;53(1):21-7. doi: 10.1111/j.1740-8261.2011.01863.x.

Valli VE, Bienzle D, Meuten DJ. Tumors of the Hemolymphatic System. In: Meuten DJ, editor. Tumors in Domestic Animals. Fifth ed. Iowa, USA: John Wiley & Sons, Inc.; 2017. p. 248.

Wang Y, Liang KR, Liu XG, Wang JA, Kang JH, Liang MZ. Relationship between peripheral lung cancer and the surrounding bronchi, pulmonary arteries, pulmonary veins: a multidetector CT observation. Clin Imaging. 2011;35(3):184-92. doi: 10.1016/j.clinimag.2010.05.001.

Wang Z, Kim J, Zhang P, Galvan Achi JM, Jiang Y, Rong L. Current therapy and development of therapeutic agents for lung cancer. Cell Insight. 2022;1(2), 100015, ISSN 2772-8927. https://doi.org/10.1016/j.cellin.2022.100015.

Wilson DW. Tumors of the Respiratory Tract. In: Meuten DJ, editor. Tumors in Domestic Animals. Fifth ed. Iowa, USA: John Wiley & Sons, Inc.; 2017a. p. 480-481.

Wilson DW. Tumors of the Respiratory Tract. In: Meuten DJ, editor. Tumors in Domestic Animals. Fifth ed. Iowa, USA: John Wiley & Sons, Inc.; 2017b. p. 486.

Wilson DW. Tumors of the Respiratory Tract. In: Meuten DJ, editor. Tumors in Domestic Animals. Fifth ed. Iowa, USA: John Wiley & Sons, Inc.; 2017c. p. 487.

Wilson DW. Tumors of the Respiratory Tract. In: Meuten DJ, editor. Tumors in Domestic Animals. Fifth ed. Iowa, USA: John Wiley & Sons, Inc.; 2017d. p. 488.

Wilson DW. Tumors of the Respiratory Tract. In: Meuten DJ, editor. Tumors in Domestic Animals. Fifth ed. Iowa, USA: John Wiley & Sons, Inc.; 2017e. p. 489.

Wilson DW. Tumors of the Respiratory Tract. In: Meuten DJ, editor. Tumors in Domestic Animals. Fifth ed. Iowa, USA: John Wiley & Sons, Inc.; 2017f. p. 496.

Withers SS, Johnson EG, Culp WT, Rodriguez CO Jr, Skorupski KA, Rebhun RB. Paraneoplastic hypertrophic osteopathy in 30 dogs. Vet Comp Oncol. 2015;13(3):157-65. doi: 10.1111/vco.12026.

Xiang W, Xing Y, Jiang S, Chen G, Mao H, Labh K, et al. Morphological factors differentiating between early lung adenocarcinomas appearing as pure ground-glass nodules measuring

≤10 mm on thin-section computed tomography. Cancer imaging. 2014;14(33), https://doi.org/10.1186/s40644-014-0033-x.